BIOCHEMICAL PHARMACOLOGY 75 (2008) 1065–1075

available at www.sciencedirect.com

ScienceDirect

journal homepage: www.elsevier.com/locate/biochempharm

Priming by lipopolysaccharide exaggerates acute lung injury and mortality in responses to peptidoglycan through up-regulation of Toll-like receptor-2 expression in mice

Naoyuki Matsuda [a], *Hiromi Yamazaki* [a], *Ken-ichi Takano* [a], *Kazuhiro Matsui* [b], *Yasuo Takano* [c], *Osamu Kemmotsu* [d], *Yuichi Hattori* [a,*]

[a] *Department of Molecular and Medical Pharmacology, Graduate School of Medicine and Pharmaceutical Sciences, University of Toyama, Sugitani 2630, Toyama 930-0194, Japan*

[b] *Department of Legal Medicine, Graduate School of Medicine and Pharmaceutical Sciences, University of Toyama, Toyama 930-0194, Japan*

[c] *Department of Diagnostic Pathology, Graduate School of Medicine and Pharmaceutical Sciences, University of Toyama, Toyama 930-0194, Japan*

[d] *Department of Anesthesiology and Critical Care Medicine, Hokkaido University, Graduate School of Medicine, Sapporo 060-8638, Japan*

ARTICLE INFO

Article history:
Received 7 September 2007
Accepted 30 October 2007

Keywords:
Peptidoglycan
Lipopolysaccharide
Toll-like receptors
Acute lung injury
Nuclear factor-κB
Transcription factor decoy
Sepsis

ABSTRACT

Invasive infection mixed with Gram-positive and Gram-negative bacteria often results in severe sepsis and septic shock, the prognosis of which is extremely poor and the mortality is high. Here, we hypothesized that lipopolysaccharide (LPS) from Gram-negative bacteria may exert a priming effect on the innate immune response to peptidoglycan (PepG) from Gram-positive bacteria and if so, examined the molecular mechanism of this priming. We found that mice who underwent intratracheal instillation with PepG (5 mg/kg) following prior administration of LPS (5 mg/kg) had a marked decline in survival as compared with the animals given each bacterial cell wall component alone. Furthermore, blood gas exchange impairment and pulmonary vascular hyperpermeability were greatly enhanced in mice given PepG after LPS stimulation, indicating a severe development of acute lung injury. LPS significantly up-regulated the expression levels of Toll-like receptor (TLR)-2 mRNA and protein in mouse lungs. Translocation of TLR-2 to the membranes was also increased by LPS stimulation. This was supported by immunohistochemical examination showing that TLR-2 expression was changed from the cytoplasm to the luminal surface of bronchiolar epithelial cells following LPS stimulation. We also demonstrated an LPS-induced increase in TLR-2 mRNA expression in type-II pneumocytes by reverse transcription-polymerase chain reaction following laser-assisted microdissection. In vivo transfection of nuclear factor-κB (NF-κB) oligonucleotides strongly prevented the up-regulation of TLR-2 after LPS stimulation at pulmonary cellular and tissue levels. We conclude that the priming effect of LPS on PepG-induced lung injury and death is preceded by NF-κB-mediated up-regulation of TLR-2.

* *Corresponding author*. Tel.: +81 76 434 7260; fax: +81 76 434 5021.
E-mail address: yhattori@med.u-toyama.ac.jp (Y. Hattori).

Abbreviations: TLR, Toll-like receptor; LPS, lipopolysaccharide; PepG, peptidoglycan; NF-κB, nuclear factor-κB; ODN, oligodeoxynucleotide; GAPDH, glyceraldehydes-3-phosphate dihydrogenase; PBS, phosphate-buffered saline; RT-PCR, reverse transcription-polymerase chain reaction; IRAK, interleukin-1 receptor-associated kinase; TRAF, tumor necrosis factor-associated factor; IKK, inhibitor of nuclear factor-κB kinase.

0006-2952/$ – see front matter
doi:10.1016/j.bcp.2007.10.036

1. Introduction

Activation of Toll-like receptors (TLRs) plays a crucial role in triggering of the innate immune response to bacterial infection. TLRs recognize pathogen-associated molecular patterns present in microbial components [1]. By now ten mammalian TLRs have been identified, with different ligand specificities [2]. Among this family of receptors, TLR-2 and TLR-4 have received great attention. TLR-4 is essential for the recognition of lipopolysaccharide (LPS), a major component of Gram-negative bacteria [3], in cooperation with MD-2, a small accessory protein which associates with extracellular domain of TLR-4 [4]. TLR-2 recognizes a large number of microbial components, including peptidoglycan (PepG) and lipoteichoic acid from Gram-positive bacteria [5,6]. Recent work has shown that PepG also signals via the intracellular pattern recognition receptor Nod2 [7].

Interferon-γ or bacteria such as *Propionibacterium acnes* can enhance the LPS-induced inflammatory response by a selective priming of mononuclear phagocytes and fibroblasts [8–10]. Quite recently, we have also reported that acute pancreatitis aggravates the LPS-induced development of acute lung injury in mice by increasing the transcript level of macrophage migration inhibitory factor [11]. Those priming effects appear to be mediated by up-regulation of TLR-4 and/or other downstream signaling molecules. As an important characteristic of PepG and its structural subunit muramyl dipeptide, their ability to enhance LPS signaling and augment its toxicity has been suggested [12–16]. This synergistic interaction has been demonstrated in respect to the release of tumor necrosis factor-α and interleukin-6 in whole human blood [12,13], the release of proinflammatory cytokines from human monocytic cell lines [15,16], and the degree of shock and multiple organ dysfunction in a rodent model of sepsis [14]. In the meantime, PepG exhibits a number of endotoxic properties [17] and has recently been shown to cause organ dysfunction when administered to rats [18]. To date, however, whether LPS has a priming effect on the systemic inflammatory response to PepG has not been studied. Furthermore, despite the reports that monocyte expression of CD14 and TLR-4 is up-regulated by exposure to LPS [19,20], the regulation of TLR-2 expression by LPS is poorly understood.

Hence, the present study initially examined the effect of PepG challenge following administration of LPS on survival in mice. We found that mice challenged with PepG following LPS had a marked decline in survival with severe acute lung injury in comparison with the animals given each bacterial cell wall component alone. We thus wished to determine whether such a priming effect of LPS on PepG toxicity is associated with up-regulated expression of TLR-2 in mouse lungs and to investigate further the regulatory mechanism of TLR-2 expression.

2. Materials and methods

2.1. Experimental animals

This study was approved by the Animal Care and Use Committee of University of Toyama. Care and handling of the animals were in accord with National Institutes of Health guidelines. Male BALB/c mice, 8–12 weeks of age, were quarantined in quiet, humidified, light-cycled rooms for 2–3 weeks before use. Mice were allowed ad libitum access to food and water throughout quarantine.

Under anesthesia with gaseous diethyl ether, the trachea was exposed through a midline incision in the anterior neck, and a 27-gauge needle was inserted. Then, the animals received intratracheal administration of LPS (5 mg/kg; *E. coli* 055:B5; List Biological Laboratories, Campbell, CA), PepG (5 mg/kg; *Staphylococcus aureus*; Sigma-Aldrich Company Ltd., St. Louis, MO) or an equal volume of sterile saline (300 μl) under direct visualization. This was done with multiple injections during each inspiration of the animal spontaneously breathing. The wound was closed after the last intratracheal injection, and the animals were allowed to recover.

Nuclear factor-κB (NF-κB) decoy delivery was performed immediately after PepG administration and was based on a protocol described previously [21]. The following sequences of phosphorothioate double-stranded oligodeoxynucleotide (ODN) against NF-κB binding site and of scrambled ODN were utilized in this study, which were the same as reported previously [22]; 5′-CCTTGAAGGGATTTCCCTCC-3′ and 3′-GGAACTTCCCTAAAGGGAGG-5′ for NF-kB decoy ODN (consensus sequences are underlined); 5′-TTGCCGTACCTGACTTAGCC-3′ and 3′-AACGGCATGGACTGAATCGG-5′ for scrambled decoy ODN. The accuracy of NF-κB decoy delivery into the lung was confirmed by the gel shift assay showing that transfection of NF-κB decoy ODN via intratracheal injection resulted in a strong reduction in the increased NF-κB activity in nuclear extracts from lungs 10 h after administration of the large dose (10 mg/kg) of LPS [23].

2.2. Survival studies

Mice were randomly divided into three groups. The first group received only intratracheal injection of 5 mg/kg LPS, the second group was subjected to coadministration of 5 mg/kg LPS and 5 mg/kg PepG, and the last group underwent 5 mg/kg LPS followed by administration of 5 mg/kg PepG 5 h later. Additional mice were given only intratracheal injection of 5 mg/kg PepG. All groups of mice were followed for survival for 3 days, during which the animals were allowed free access to food and water.

2.3. Pulmonary microvascular leakage

Pulmonary vascular permeability was assessed by Evans blue dye extravasation as described by Sirois et al. [24]. In brief, Evans blue dye (20 mg/kg) was given intravenously to mice 10 min before the animals were sacrificed. Thereafter, the chest cavity was opened, and the animals were perfused, via a catheter implanted through the right ventricle up to the pulmonary artery, with 15 ml of phosphate-buffered saline (PBS) for 1 min. Right pulmonary inferior lobes were harvested, weighed and divided in two equal sections. One was immersed in formamide (4 ml/g wet weight) at room temperature for 24 h for the extraction of the dye and the other was put to dry in oven (60 °C) till constant weight. The absorbance of Evans blue dye extracted in formamide was then measured by spectrophotometry at a wavelength of 620 nm using a plate reader. The concentration of the dye was then calculated from a standard curve and expressed as μg of Evans blue per g of dry tissue.

2.4. Poly(A)$^+$ RNA purification and Northern blot analysis

Total RNA was extracted from lung tissues by the guanidinium thiocyanate–phenol–chloroform method with Isogen (Nippon Gene, Toyama, Japan) used routinely in our laboratory [25]. Then, Poly(A)$^+$ RNA was purified from total RNA using a GenElute^{TM} mRNA Miniprep Kit (Sigma–Aldrich), and the amount of extracted Poly(A)$^+$ RNA was determined by UV absorption. Northern blot was performed as described previously [26] with slight modifications. In brief, samples (20 μg) were electrophoresed on agarose/formaldehyde gels and transferred to a Hybond-N$^+$ nylon membrane (Amersham Biosciences, Little Chalfont, Buckinghamshire, UK). The filter was baked, prehybridized, and hybridized with ^{32}P-labeled oligonucleotides or full-length cDNA for target molecules. The intensity of hybridization was visualized by autoradiography. Expression of mRNA was quantitated by counting the radioactivity using a Bioimaging Analyzer (Fujix BAS 2000; Fuji Photo Film, Tokyo, Japan). To control for differences in RNA content, the membranes were sequentially probed for glyceraldehydes-3-phosphate dihydrogenase (GAPDH) after stripping. Thus, the amount of target molecule mRNA was normalized to the mRNA of the constitutively expressed protein GAPDH on the same filter.

2.5. Western blot analysis

The nuclear and membrane fractions were prepared from lung tissues using methods described previously [23,25]. Samples (2–20 μg) were run on SDS-PAGE (7.5% polyacrylamide gel) and electrotransferred to a polyvinylidine difluoride filter membrane. To reduce nonspecific binding, the membrane was preincubated for 60 min at room temperature in PBS (137 mM NaCl, 2.7 mM KCl, 8.1 mM Na_2HPO_4, and 1.5 mM KH_2PO_4) containing 1% bovine serum albumin. The membrane was then incubated for 120 min at room temperature with primary antibody recognizing NF-κB subunit of p65, TLR-2 or actin. We used the following commercially available antibodies: anti-rabbit IgG-p65 antibody (GeneTex, San Antonio, TX), anti-rabbit IgG-TLR-2 antibody (Acris, Hiddenhausen, Germany), and anti-rabbit IgG-actin antibody (GeneTex). After an extensive washing with PBS containing 0.05% Tween 20, the membrane was incubated with horseradish peroxidase-conjugated anti-rabbit IgG antibody (eBioscience, San Diego, CA) diluted at 1:1000 in PBS-Tween 20 buffer at room temperature for 60 min. The blots were washed twice in PBS-Tween 20 buffer and subsequently visualized with an enhanced chemiluminescence detection system (Amersham), exposed to X-ray film, and analyzed by NIH image software produced by Wayne Rasband (National Institutes of Health, Bethesda, MD). Intensity of total protein bands per lane was evaluated by densitometry. Negligible loading/transfer variation was observed between samples.

2.6. Electrophoretic mobility shift assay

For the detection of NF-κB DNA binding activity, double-stranded oligonucleotides with consensus sequences of NF-κB (5′-AGT TGA GGG GAC TTT CCC AGG C-3′) were purchased from Santa Cruz Biotechnology (Santa Cruz, CA). The oligonucleotides were end labeled in 10 μl of reaction buffer (in mM: 50 Tris–HCl (pH 8.0), 10 $MgCl_2$, and 5 dithiothreitol) along with T4 polynucleotide kinase and [γ-^{32}P]ATP (4500 Ci/mmol at 10 μCi/μl; MP Biomedicals; Solon, OH) for 30 min at 37 °C as recommended by the manufacturer (Takara Shuzo, Ohtsu, Japan). The DNA binding reaction was conducted in a volume of 15 μl. The reaction mixture contained 20 μg nuclear extract, 10 mM Tris–HCl (pH 7.5), 40 mM NaCl, 1 mM EDTA, 4% (v/v) glycerol, 0.5 mM $MgCl_2$, 1 mM dithiothreitol, and 0.06 mg/ml poly(dI-dC). Labeled probe (~30,000 c.p.m.) was then added, and the binding reaction was incubated for 30 min at room temperature. After adding bromophenol blue and xylene cyanol, samples were loaded onto a 5% polyacrylamide gel and run at 100 V for ~60 min. Gels were then dried under vacuum and subjected to autoradiography.

2.7. Immunohistochemistry

Under deep anesthesia with sodium pentobarbital, midsternal thoracotomy was performed, and lungs were perfused with PBS through the left ventricle and fixed with 4% buffered formalin solution. Lungs were carefully excised, avoiding any damage, placed in 4% buffered formalin solution for 6 h at 4 °C, immersed in PBS containing 30% sucrose overnight, and frozen in liquid nitrogen. Sections 10 μm in thickness were cut from frozen tissues, mounted on poly-L-lysin-coated glass slides, and treated with 0.3% Triton X-100 in PBS for 1 h. Endogenous peroxidase activity was quenched by incubation in 1% hydrogen peroxide diluted in methanol for 15 min. After being blocked by normal goat serum to prevent nonspecific staining by the secondary antibody, the sections were incubated with anti-rabbit IgG-TLR-2 antibody overnight at room temperature, followed by exposure to biotinylated goat anti-rabbit IgG (Nichirei, Tokyo, Japan) and then to streptavidin peroxide (Nichirei), each for 1 h. Bound antibody was visualized by a light microscopy with 0.01% diaminobenzidine and 0.002% hydrogen peroxide. The specificity of the immunoreaction was evaluated in comparison with the negative control specimen in which nonimmune IgG was used instead of the primary antibody.

2.8. Tissue microdissection and RNA extraction

Lungs were gently harvested, the trachea was cannualated, and lungs were fixed using methanol-based UMFIX reagent (Sakura Finetek Japan, Tokyo, Japan). Then, lung tissues were sectioned at a thickness of 100 μm and microdisected by using the Leica DMLA laser capture microscope (Leica Microsystems, Bannockburn, IL). Cells from alveolar regions were dissected out and the cut-out pieces were placed directly into tubes containing the lysis buffer supplied in GenElute^{TM} Mammalian Total RNA Kit (Sigma–Aldrich). The total RNA was extracted and purified by the use of the GenElute^{TM} mRNA Miniprep Kit (Sigma–Aldrich) according to the manufacturer's instructions.

2.9. Reverse transcription-polymerase chain reaction (RT-PCR)

The quality of the extracted RNA was determined by UV absorption in which the optical density (OD) ratio of

$OD_{280\ nm}$:$OD_{260\ nm}$ was calculated. RT-PCR was performed by using primers derived from the mouse TLR-2 sequence. The oligonucleotide sequence pair used for gene amplification in this study generated PCR products of expected size that has been sequenced to verify TLR-2 identity: sense primer, 5′-TGCTTTCCTGCTGGAGATTT-3′ and antisense primer, 5′-TGTAACGCAACAGCTTCAGG-3′ (197 bp). cDNA was reverse transcribed from 0.5 μg total RNA according to the manufacture's instructions of an RT-PCR kit (Takara Shuzo). The PCR conditions were 35 cycles of denaturation at 85 °C for 30 s, annealing at 60 °C for 30 s, and extension at 72 °C for 30 s. After amplification, the resulting PCR products visualized on 2% agarose gels stained with ethidium bromide. To standardize the amount of the target molecule, the amount of GAPDH mRNA, a ubiquitously expressed housekeeping gene was determined with the primer pair (sense, 5′-CCTGTGGGTTGTGACCTCTT-3′, and antisense, 5′-TTGTGTTCTCAGCCATCTGC-3′; 218 bp).

2.10. Statistical analysis

Data are expressed as means ± S.E.M. Data were analyzed using the StatView II program (Abacus Concepts, Berkeley, CA). Statistical analysis was performed using Student's *t*-test or a repeated-measure one-way analysis of variance followed by Bonferroni's multiple comparison test when appropriate; a *P* value less than 0.05 was considered significant.

3. Results

3.1. Survival after challenge with intratracheal LPS and PepG

In the initial studies, mice underwent intratracheal instillation with LPS (5 mg/kg) and/or PepG (5 mg/kg). All animals survived after administration of PepG alone. Additionally, mortality was only 10% at 3 days after LPS alone was challenged. As shown in Fig. 1, however, 40% of the animals which received coadministration of LPS and PepG died within 36 h, and the survival plateaued for an additional 2 days. On the other hand, when PepG was given 5 h after LPS administration, mortality was more progressive with 70% of the animals being deceased within 24 h.

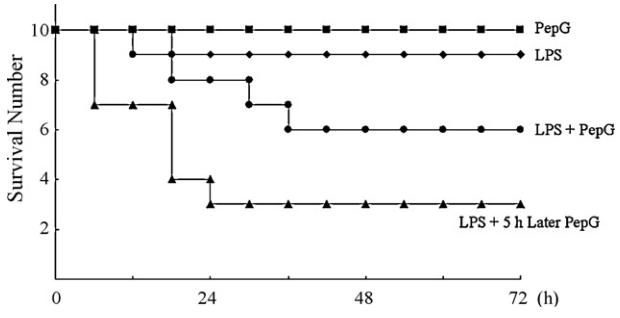

Fig. 1 – Kaplan–Meier survival curves. No deaths occurred in mice that underwent intratracheal instillation with PepG (5 mg/kg) alone. After LPS (5 mg/kg) alone was intratracheally given, only one of the animals died during the observation period. When PepG was given concurrently with or at 5 h after LPS administration, the animals exhibited lethality. The mortality was monitored four times daily for 3 days. Ten mice were used for each group.

3.2. Acute lung injury

Table 1 summarizes the values for blood gases in mice after intratracheal administration of LPS and/or PepG. When the animals were given LPS or PepG alone, the blood gas parameters were not much different from the control values. Coadministration of LPS and PepG resulted in significant decreases in arterial PO_2, pH and base excess. However, such changes were not so pronounced. A severe hypoxemic condition was induced by administration of PepG 5 h after LPS stimulation, as indicated by markedly reduced arterial PO_2 in comparison with the control value. Furthermore, mice who received LPS and 5 h later received PepG exhibited a profound decrease in arterial blood pH and a greatly lowered value for base excess, indicating metabolic acidosis.

When pulmonary microvascular leakage was assessed by Evans blue dye extravasation, intratracheal administration of LPS and PepG alone caused only a 2.9- and 2.4-fold increase in lung vascular permeability, respectively, at 7 h after challenge ($n = 5$ for each group). A further increase was observed at 7 h following coadministration of LPS and PepG (4.5-fold, $n = 5$). The effect of intratracheal instillation with PepG 5 h following LPS stimulation was more striking: lung vascular permeability was increased 7.2-fold after 2 h ($n = 5$).

3.3. NF-κB activation

To examine the activation of NF-κB in mouse lungs, we measured NF-κB translocation to the nucleus with the antibody to an NF-κB subunit of p65. As presented in Fig. 2A, translocation of NF-κB to the nucleus was increased 3.6-fold in lungs from mice 7 h after intratracheal administration of PepG. A similar increase in NF-κB nuclear translocation was found at 7 h after LPS alone was intratracheally given (4.2 ± 0.3 fold, $n = 5$). This increase in NF-κB nuclear translocation was more marked in lungs from mice 7 h after coadministration of LPS and PepG (7.4-fold). Furthermore, a 14.3-fold increase in NF-κB nuclear translocation in lungs was found at 2 h after the animals received LPS and 5 h later received PepG. Transfection of NF-κB decoy ODN, which was intratracheally instilled 5 h after LPS, resulted in a significant inhibition of the dramatic increase in NF-κB nuclear translocation induced by PepG administration following LPS. Additionally, analysis of NF-κB binding activity was performed in nuclear protein extracts from lungs by gel mobility shift assays (Fig. 2B). PepG challenge led to an evident increase in NF-κB binding activity. In lungs from the animals given PepG 5 h after LPS treatment, there was a tendency toward a further increase in activity of NF-κB binding. This increase in NF-κB binding activity was strongly inhibited by in vivo transfection of NF-κB decoy ODN. The addition of excess unlabeled NF-κB oligonucleotides competed with labeled NF-κB probe, demonstrating the specificity of the protein/DNA interaction (Fig. 2B, lane 7).

Table 1 – Blood gases in mice

	PaO_2 (mmHg)	$PaCO_2$ (mmHg)	pH	Base excess (mM)
Control	109.7 ± 2.7	36.7 ± 1.4	7.41 ± 0.01	−0.1 ± 0.1
LPS	98.3 ± 2.4	34.3 ± 1.2	7.31 ± 0.01	−2.9 ± 0.1*
PepG	101.2 ± 2.8	33.8 ± 0.9	7.32 ± 0.00	−2.2 ± 0.3
LPS + PepG	83.7 ± 1.7*	32.4 ± 1.2	7.28 ± 0.01*	−4.9 ± 0.3*
PepG after LPS	56.8 ± 3.1*	31.8 ± 1.2	7.14 ± 0.05*	−11.6 ± 1.0*

The values are expressed as means (±S.E.M.; $n = 4$). At 7 h after LPS (5 mg/kg), PepG (5 mg/kg) or LPS + PepG, or at 2 h after PepG 5 h following LPS, mice were anesthetized with gaseous diethyl ether, the blood samples were collected by cardiac puncture for blood gas analysis.
* Significant difference from vehicle-treated control values.

3.4. *LPS-induced TLR-2 overexpression and membrane translocation*

Northern blot analysis using the TLR-2 probe revealed a major mRNA species of 3 kb in mouse lung tissues (Fig. 3A). At 5 h following intratracheal administration of LPS, TLR-2 mRNA was markedly increased. Because the bioimaging analysis of Northern blots indicated that GAPDH mRNA was unaffected by LPS (Fig. 3A), this mRNA was used as an internal standard. When normalized to GAPDH mRNA levels, a 5.5-fold increase in TLR-2 mRNA was found in lungs from mice 5 h after LPS (Fig. 3B). Transfection of NF-κB decoy ODN strongly suppressed the increase in LPS-induced TLR-2 pulmonary expression. However, the scrambled ODN decoy was without effect on TLR-2 overexpression in LPS-treated lungs.

On Western blots, the 86 kDa protein of TLR-2 was markedly increased by LPS challenge in lungs (Fig. 4A). Densitometric quantification of the signal showed that the expression level of TLR-2 in the total fraction of 5-h endotoxemic lungs was 5.3-fold higher than in controls

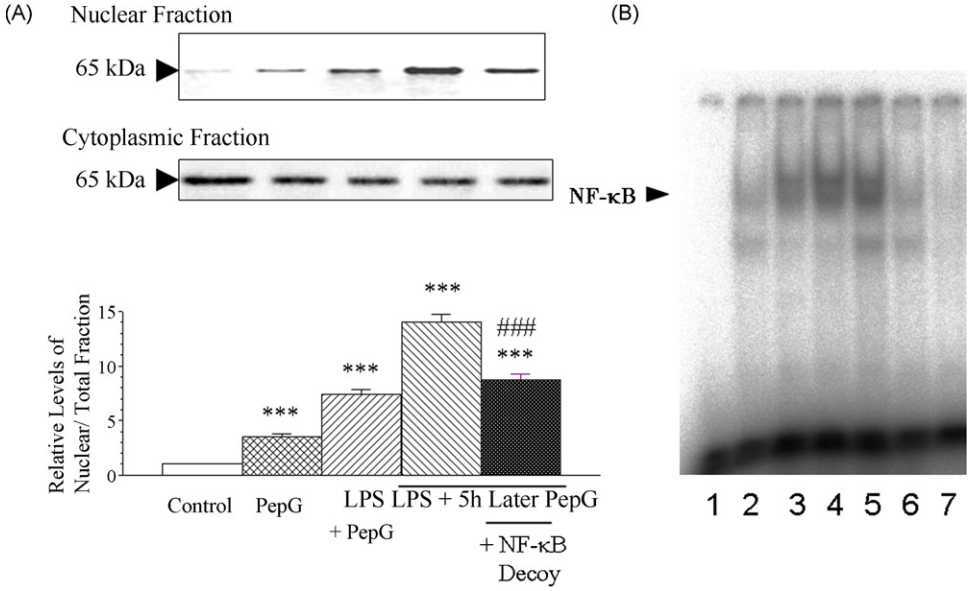

Fig. 2 – Effects of intratracheal instillation with LPS (5 mg/kg) and/or PepG (5 mg/kg) on NF-κB activation in mouse lungs. At 7 h after administration of PepG alone, at 7 h after coadministration of PepG and LPS, and at 2 h after administration of PepG following 5 h of LPS stimulation, nuclear and cytoplasmic fractions were obtained from the lungs. Both extracts were prepared for analysis of NF-κB p65 protein by Western blot (A) and the nuclear extracts were for NF-κB binding activity by electrophoretic mobility shift assay (B) as described in Section 2. Transfection of NF-κB decoy ODN was intratracheally instilled concurrently with PepG at 5 h after LPS administration. In panel A, traces represent typical Western blots showing immunochemical detection as a 65 kDa band. Bands were quantified in arbitrary units by densitometry. In each of the experiments, the protein expression level obtained from the control band is normalized as 1.0. Values are expressed as means (±S.E.M.; $n = 5$). $^{***}P < 0.001$ compared with the control group. $^{\#\#\#}P < 0.001$ compared with the group that received PepG following LPS. In panel B, the induced NF-κB shift bands are indicated. Lane 1, free probe showed no detection of NF-κB binding activity; lane 2, nuclear extracts from control mouse lung tissues were incubated with a ^{32}P-labeled NF-κB probe; lane 3, nuclear extracts were taken from lungs of the mouse given PepG alone; lane 4, nuclear extracts were taken from lungs of the mouse after coadministration of LPS and PepG; lane 5, nuclear extracts were taken from lungs of the mouse given PepG at 5 h after LPS; lane 6, nuclear extracts from lung tissues of the mouse that was transfected with NF-κB decoy ODN concurrently with PepG at 5 h after LPS were incubated with a ^{32}P-labeled NF-κB probe; lane 7, nuclear extracts from lung tissues of the mouse given PepG following LPS were incubated with a ^{32}P-labeled NF-κB probe in the presence of excess unlabeled NF-κB oligonucleotides. Results shown are representative of three independent experiments.

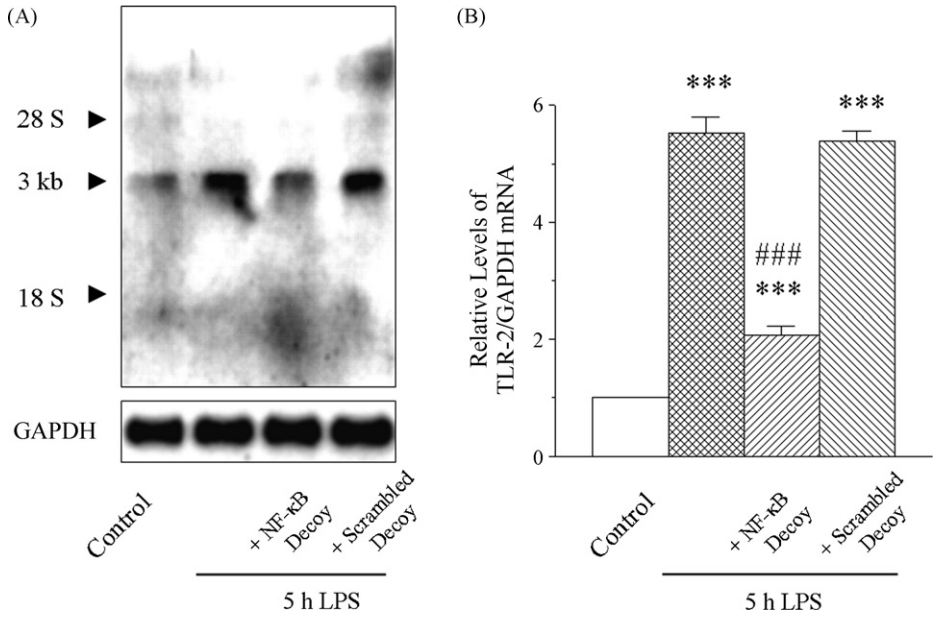

Fig. 3 – Northern blot analysis of TLR-2 mRNA expression in lungs from mice that were vehicle treated, 5-h LPS (5 mg/kg) treated, and transfected with NF-κB decoy ODN or its scrambled form after LPS treatment. Panel A: representative autograph of Northern blot analysis of TLR-2 mRNA and GAPDH mRNA expression. TLR-2 mRNA was detected as a single major band of 3 kb. The location of ribosomal RNA (28 S and 18 S) is indicated. GAPDH mRNA was unaffected by LPS treatment. Panel B: summary of quantification of densitometric measurement as ratio of TLR-2 mRNA relative to GAPDH mRNA. Values are expressed as means (±S.E.M.; $n = 5$). $^{***}P < 0.001$ compared with the control (vehicle-treated) group. $^{###}P < 0.001$ compared with LPS treatment alone.

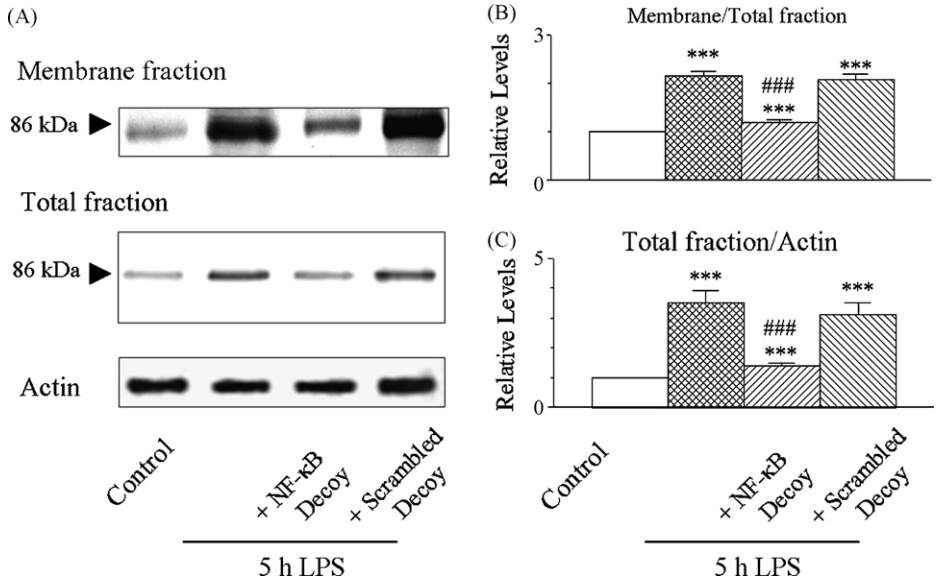

Fig. 4 – Protein expression and membrane translocation of TLR-2 in lungs from mice that were vehicle treated, 5-h LPS (5 mg/kg) treated, and transfected with NF-κB decoy ODN or its scrambled form after LPS treatment. Panel A: representative immunoblots of TLR-2 in the total fraction (top) and in the membrane fraction (bottom), and of actin (middle) in the total fraction, which served as loading control. TLR-2 was immunochemically detected as an 86-kDa band. Panel B and C: bar graphs summarizing the immunoblot data. Bands were quantified in arbitrary units by densitometry. Values are means (±S.E.M.; $n = 5$) of TLR-2/actin (B) and of TLR-2 in membrane/total fractions (C) expressed relative to the respective control result which is normalized as 1.0. $^{***}P < 0.001$ compared with the control (vehicle-treated) group. $^{###}P < 0.001$ compared with LPS treatment alone.

(Fig. 4B). Moreover, the TLR-2 level in the membrane fraction was dramatically increased 5 h after intratracheal administration of LPS (Fig. 4A and C). The LPS-induced increases in the protein expression level and translocation to the membrane pool of TLR-2 were greatly inhibited by trasfection of NF-κB decoy ODN, but not of its scrambled form.

3.5. *Immunohistochemical localization and intensity of TLR-2 expression in lung tissues*

After periodical induction of lung tissue damage by intratracheal administration of LPS and PepG, characteristic changes in immunohistochemical localization and intensity of TLR-2 expression in bronchiolar epithelial cells were observed. In the control group, TLR-2 was restricted in the nuclei of bronchiolar epithelial cells and faint expression was recognized in the cytoplasm (Fig. 5A). However, 2 h after LPS administration TLR-2 expression was observed in the luminal surface of bronchiolar epithelial cells, especially in Clara cells with hobnail morphology, in addition to its expression in the nuclei and cytoplasm (Fig. 5B). Furthermore, this expression increased more markedly 5 h after LPS (Fig. 5C). In contrast, 6 h after the second hit of PepG following LPS TLR-2 expression in the nuclei and cytoplasm was greatly attenuated but remained strong in the luminal surface of bronchiolar epithelial cells (Fig. 5D). TLR-2 expression was also observed to a certain extent in the endothelial cells of the vessels beneath bronchioles. PepG alone failed to induce the shift of TLR-2 expression to the luminal surface as seen in lung sections from the animals treated with PepG following LPS (data not shown).

Expression of TLR-2 in the alveolar areas was analyzed. TLR-2 was expressed weakly in the nuclei of type-I and type-II pneumocytes in the control (Fig. 6A), but 5 h after LPS administration its expression increased strongly in the nuclei of endothelial cells besides type-I and type-II pneumocytes (Fig. 6B). Likewise, some cells exhibited more intense cellular surface expression of TLR-2.

3.6. *Gene expression of TLR-2 in type-II pneumocytes*

We used laser capture microdissection to collect type-II pneumocytes from frozen sections of lungs of mice subjected to intratracheal LPS. The RNA from these cells was harvested for analysis of TLR-2 mRNA by RT-PCR. TLR-2 mRNA in type-II pneumocytes was increased 9.5-fold at 5 h after intratracheal administration of LPS. This increase in TLR-2 mRNA was markedly suppressed by NF-κB decoy ODN. However, the scrambled ODN decoy had no effect on LPS-induced up-regulation of TLR-2 mRNA (Fig. 7).

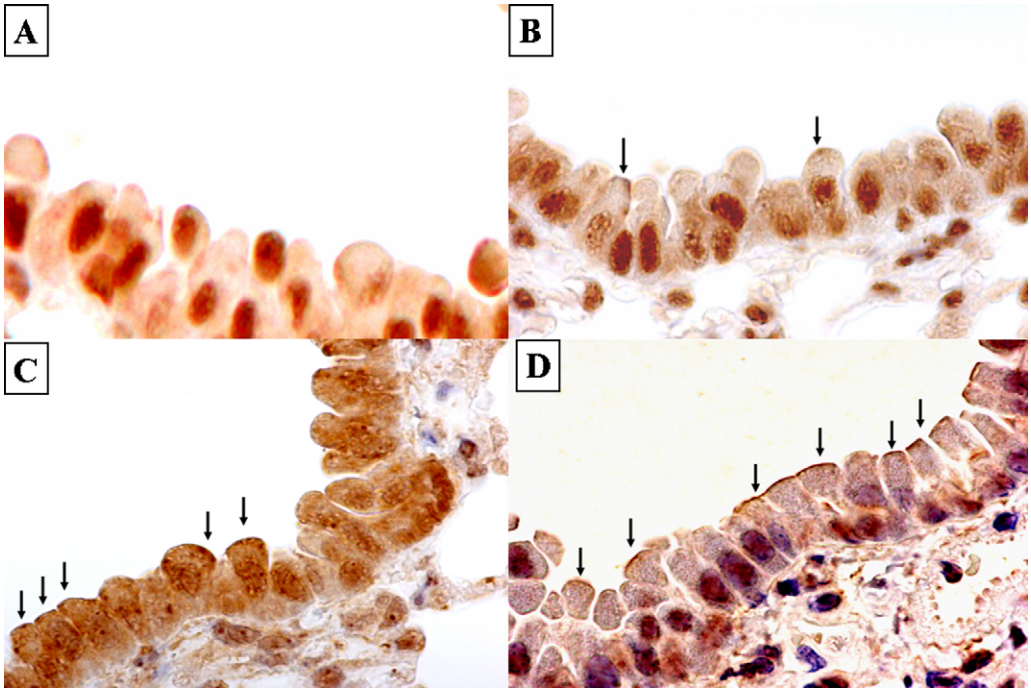

Fig. 5 – Immunohistochemical localization and intensity of TLR-2 expression in bronchiolar epithelial cells (A: control mouse; B and C: mouse at 2 h and 5 h after 5 mg/kg LPS was intratracheally administered, respectively; D: mouse at 6 h after 5 mg/kg PepG was intratracheally administered following 5 h of LPS). In the control, strong TLR-2 expression was restricted in the nuclei while faint expression in the cytoplasm of bronchiolar epithelial cells (A). At 2 h after LPS, TLR-2 expression was weak in the cytoplasm, relatively strong in the luminal surface, especially in Clara cells with hobnail morphology (arrows) and granular like staining in the nuclei of bronchial epithelial cells were visible (B). At 5 h after LPS, TLR-2 expression greatly increased in the nuclei, cytoplasm, and luminal surface of bronchiolar epithelial cells (arrows) (C). At 6 h after second hit of PepG following LPS, TLR-2 was strongly attenuated in the both nuclei and cytoplasm but remained in the luminal surface, and positive staining was also found in vascular endothelial cells (D) (immunohistochemistry with Mayer's hematoxylin conterstein, ABC methods; original magnification, each ×40).

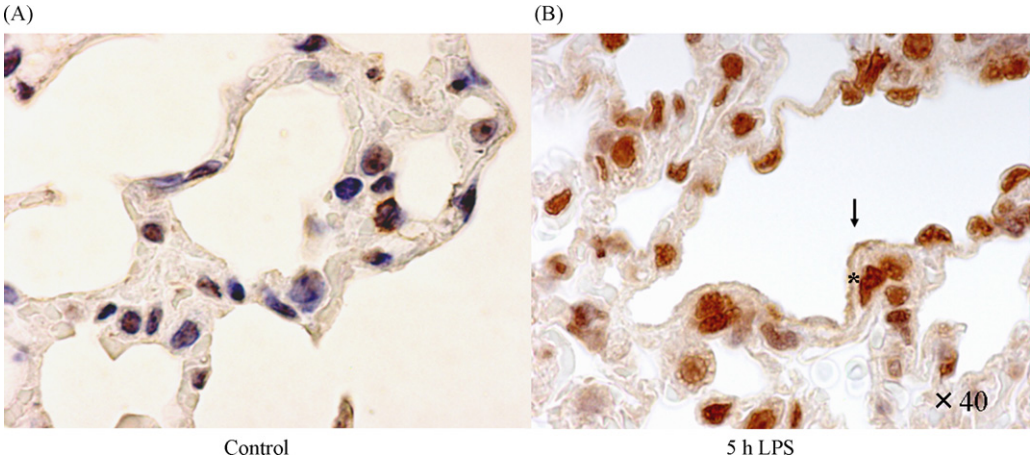

Fig. 6 – Immunohistochemical localization and intensity of TLR-2 expression in alveolar epithelial cells (A: control mouse; B: mouse at 5 h after 5 mg/kg LPS was intratracheally administered). TLR-2 expression was weak in the nuclei of type-I and type-II pneumocytes in the control (A), whereas it markedly increased in the nuclei of epithelial cells as well as type-I and type-II pneumocytes (arrow) following LPS (B). Some cells revealed intense cellular surface staining (*) (immunohistochemistry with Mayer's hematoxylin conterstein, ABC methods; original magnification, each ×40).

4. Discussion

We investigated the potential role of the regulation of TLR-2 in the phenomenon of priming by LPS for the enhanced inflammatory response to PepG, a reactive ligand for TLR-2, in mice. Intratracheal administration of a small dose (5 mg/kg) of LPS or PepG alone caused only modest lung inflammation and exerted no lethal effect. Coadministration of LPS and PepG had a significantly injurious effect on lungs and increased lethality, but more striking deterioration was found when mice received LPS and 5 h later received PepG. Indeed, although blood gas analysis showed a significant decrease in PO_2 levels when PepG was administered at the same time as LPS, this decrease was more striking with PepG following LPS priming, which could lead to peripheral anerobic metabolism, resulting in metabolic acidosis as indicated by markedly lowered base excess. This priming effect of LPS to augment PepG toxicity was associated with up-regulation of pulmonary expression of TLR-2. Our observation that LPS stimulation resulted in up-regulation of TLR-2 expression concurs with previous reports using human monocyte models. Thus, TLR-2 gene expression has been shown to increase following treatment either whole blood or cultured human monocytes with LPS [27,28]. Moreover, LPS challenge of mice has been shown to cause an increase in TLR-2 mRNA in lungs [29]. Nevertheless, the present study represents the first report indicating that up-regulation of TLR-2 by LPS can lead to aggravation of acute lung injury and mortality in response to a subsequent intratracheal instillation with PepG in mice.

In invasive bacterial infection, TLRs, a family of phylogenetically conserved receptors, have attracted particular interest because of their functions in the regulation and linking of innate immune and inflammatory processes. We have found that TLR-4, a receptor for LPS which is a major cellular component of Gram-negative bacteria, is expressed in mouse lung tissues [11]. In this study, the priming with LPS stimulation of TLR-4 was significantly up-regulated expression of TLR-2 mRNA and protein in mouse lungs. TLR-2 is a receptor for several ligands such as PepG, lipoteichoic acid, lipoarabinomannan, atypical liposaccharide, heat-shock protein 70, and lipoprotein [5,30,31]. PepG is one of major proteins on the cell wall of Gram-positive bacteria. Hence, our finding that TLR-2 was up-regulated in lungs which underwent to LPS stimulation would be of significance in changes in the inflammatory reactions by microbial products in mixed bacterial infections.

In addition to overexpression of TLR-2, the data presented in this study demonstrated that the priming with LPS stimulation resulted in an increase in translocation of TLR-2 to the membranes in lung tissues. Furthermore, immunohistochemical examination showed that TLR-2 expression was changed from the cytoplasm to the luminal surface of bronchiolar epithelial cells following LPS stimulation. In quiescent lung tissues, the great part of TLR-2 appears to be present into the cytoplasm of cells. TLR-2 located on the cell surface can recognize PepG. Therefore, the up-regulation by LPS of the cell surface expression of TLR-2 could increase sensitivity to PepG and lead to enhanced activation of intracellular signaling pathways. Following activation by PepG, TLR-2 would be recruited to the lipid raft cluster, which permits the triggering of intracellular signaling cascades. Thus, recurrent intracellular localization of TLR-2 is a feature of exposure to its ligands. Activation of TLR-2 leads to the recruitment of MyD88, a cytoplasmic molecule that serves as an adaptor, which then facilitates the association of interleukin-1 receptor-associated kinase (IRAK)4 with MyD88. IRAK4 phosphorylates IRAK1, and activated IRAK1 autophosphorylates and enables tumor necrosis factor-associated factor (TRAF)6 to bind this complex. TRAF6 then disengages and translocates to the cytoplasm to activate the inhibitor of nuclear factor-κB kinase (IKK) complex and MAPKs resulting in the release of NF-κB and c-Jun N-terminal kinase [1].

Indeed, PepG was found to activate NF-κB in lungs, as indicated by increases in nuclear translocation and binding

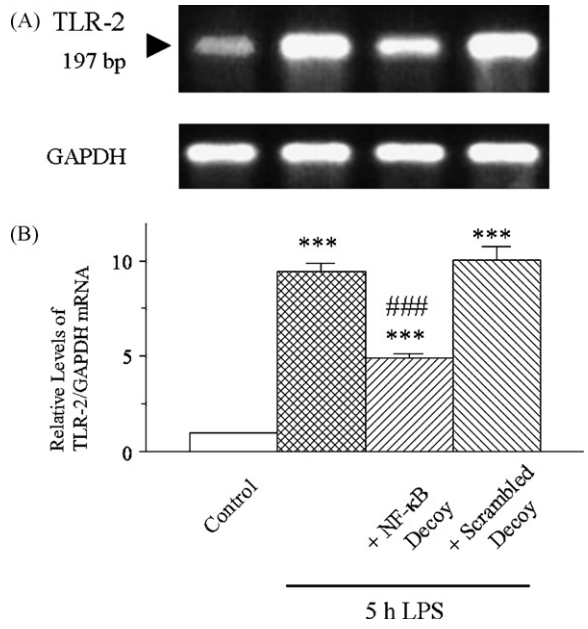

Fig. 7 – RT-PCR analysis showing gene expression of TLR-2 in type-II pneumocytes. The samples of type-II pneumocytes were microdissected from the sliced sections of lung tissues of mice that were vehicle treated, 5-h LPS (5 mg/kg) treated, and transfected with NF-κB decoy ODN or its scrambled form after LPS treatment. Panel A: representative RT-PCR of TLR-2 mRNA expression. PCR amplification product was detected at 197 bp for TLR-2. Note that there is no apparent difference in GAPDH mRNA used as an internal control among groups. Panel B: summary of quantification of densitometric measurement as ratio of TLR-2 mRNA relative to GAPDH mRNA. Values are expressed as means (±S.E.M.; $n = 3$). $^{***}P < 0.001$ compared with the control (vehicle-treated) group. $^{###}P < 0.001$ compared with LPS treatment alone.

activity of NF-κB. At the dose used in this study (5 mg/kg), however, PepG weakly induced this major proinflammatory signaling mediator. Since stimulation of TLR-4 with LPS also induces NF-κB activation in mouse lungs [11,23], LPS from Gram-negative bacteria and PepG from Gram-positive bacteria would result in activation of similar signal transduction systems. In fact, the clinical picture of sepsis caused by Gram-negative bacteria and Gram-positive bacteria is nearly identical [32]. When a small dose (5 mg/kg) of LPS was used to obtain the same modest effect as PepG, the NF-κB activating effect of co-administration of the two bacterial products appeared to be additive. However, we observed a substantial synergy on NF-κB activation when PepG was given following prior administration of LPS. This molecular basis for the priming and synergism by LPS may be associated with the up-regulation of TLR-2 mRNA and cell surface expression in lung tissues. As a result, the innate inflammatory actions in response to PepG could be coordinantly up-regulated in lungs after the priming with LPS. Thus, prior administration of LPS led to severe acute lung injury and poor survival in the animals given PepG.

The important finding in this study is that transfection of NF-κB decoy ODN prevented the LPS-induced increases in TLR-2 overexpression and membrane translocation in mouse lungs. The preventive effect of NF-κB decoy ODN transfection on LPS-up-regulated TLR-2 mRNA in type-II pneumocytes was also demonstrated by RT-PCR following laser-assisted microdissection. The successful in vivo transfer of a sufficient quantity of NF-κB decoy ODN into mouse lungs has been proven by the gel shift assay [21,23]. The specificity of the inhibitory effect of the decoy ODN against NF-κB in lungs was supported by the observation that the use of scrambled decoy ODN was without effect. These findings suggest that LPS-induced NF-κB activation is a critical mechanism of the up-regulation of TLR-2 cell surface expression in lungs. In agreement with this view, LPS has been indicated to induce TLR-2 up-regulation through TLR-4-, MyD88-, and NF-κB-dependent signaling in human endothelial cells [33]. Furthermore, it is noteworthy to describe the previous work that LPS fails to up-regulate TLR-2 mRNA in TLR-4 knockout mice [29], indicating that TLR-4 signaling mediates the LPS-induced up-regulation of TLR-2. The use of NF-κB decoy ODN not only provides evidence that expression of TLR-2 is highly regulated by NF-κB when cells are stimulated with LPS but also represents a potential strategy in the treatment of the severe septic syndrome resulting from the phenomenon of synergy in mixed bacterial infections.

Localization of TLRs has largely been associated with immune and inflammatory cells [34]. However, human airway epithelial cells have been demonstrated to express mRNAs for different TLRs [35]. Although the level of TLR-4 is low, LPS appears to be able to activate epithelial cells. Moreover, epithelial cells highly express functional TLR-2. Expression of TLR-2 mRNA and protein has been documented in human type-II alveolar epithelial cells [36,37]. In this study, we detected TLR-2 expression in bronchiolar epithelial cells of mouse lungs using immunohistochemical techniques. Within the airway, PepG administered intratracheally could activate TLR-2 on the epithelial cell surface. Interestingly, our present data suggest that type-II pneumocytes are capable of responding to PepG stimulation because of expression of TLR-2 by these cells. Thus, expression of TLR-2 by different parenchyma cells may play a crucial role in Gram-positive infectious inflammatory propagation in lungs. Hence, from the airway in response to Gram-positive pathogens, inflammatory signals and injurious damage could develop within the lung.

In conclusion, the priming effect of LPS on the PepG-induced inflammatory reaction in mice is preceded by up-regulation of TLR-2 by LPS stimulation. The up-regulation of TLR-2 by the priming with LPS was the result of activation of NF-κB, a key transcription factor regulating numerous immune and inflammatory genes. In response to intratracheal challenge with PepG following the priming with LPS, we observed an apparently synergic effect on lung injury and lethality in mice. This may be of relevance to the excess mortality observed in patients with mixed bacterial infections [38].

Acknowledgments

We thank Megumi Matsui for expert secretarial assistance. This work was supported by a grant-in-aid for Scientific

Research and for Exploratory Research from the Ministry of Education, Culture, Sports, Science and Technology of Japan.

Conflict of interest

None.

REFERENCES

[1] Akira S, Takeda K. Toll-like receptor signalling. Nat Rev Immunol 2004;4:499–511.
[2] Takeda K, Kaisho T, Akira S. Toll-like receptors. Annu Rev Immunol 2003;21:335–76.
[3] Chow JC, Young DW, Golenbock DT, Christ WJ, Gusovsky F. Toll-like receptor-4 mediates lipopolysaccharide-induced signal transduction. J Biol Chem 1999;274:10689–92.
[4] Shimazu R, Akashi S, Ogata H, Nagai Y, Fukudome K, Miyake K, et al. MD-2, a molecule that confers lipopolysaccharide responsiveness on Toll-like receptor 4. J Exp Med 1999;189:1777–82.
[5] Schwandner R, Dziarski R, Weshe H, Rothe M, Kirschning CJ. Peptidoglycan- and lipoteicholic acid-induced cell activation is mediated by toll-like receptor 2. J Biol Chem 1999;274:17406–9.
[6] Yoshimura A, Lien E, Ingalls RR, Tiomanen E, Dziarski R, Golenbock D. Cutting edge: recognition of Gram-positive bacterial cell wall components by the innate immune system occurs via Toll-like receptor 2. J Immunol 1999;163:1–5.
[7] Girardin SE, Boneca IG, Viala J, Chamaillard M, Labigne A, Thomas G, et al. Nod2 is a general sensor of peptidoglycan through muramyl depeptide (MDP) detection. J Biol Chem 2003;278:8869–72.
[8] Tamai R, Sakuta T, Matsushita K, Torii M, Takeuchi O, Akira S, et al. Human gingival $CD14^+$ fibroblasts primed with gamma interferon increase production of interleukin-8 in response to lipopolysaccharide through up-regulation of membrane CD14 and MyD88 mRNA expression. Infect Immun 2002;70:1272–8.
[9] Hayes MP, Zoon KC. Priming of human monocytes for enhanced lipopolysaccharide responses: Expression of alpha interferon, interferon regulatory factors, and tumor necrosis factor. Infect Immun 1993;61:3222–7.
[10] Romics Jr L, Dolganiuc A, Kodys K, Drechsler Y, Oak S, Velavudham A, et al. Selective priming to Toll-like receptor 4 (TLR4), not TLR2, ligands by *P. acnes* involves upregulation of MD-2 in mice. Hepatology 2004;40:555–64.
[11] Matsuda N, Nishihira J, Takahashi Y, Kemmotsu O, Hattori Y. Role of macrophage migration inhibitory pancreatitis complicated by endotoxemia. Am J Respir Cell Mol Biol 2006;35:198–205.
[12] Jørgensen PF, Wang JE, Almlöf M, Thiemermann C, Foster SJ, Solberg R, et al. Peptidoglycan and lipoteichoic acid modify monocyte phenotype in human whole blood. Clin Diagn Lab Immunol 2001;8:515–21.
[13] Wang JE, Jørgensen PF, Ellingsen E, Almlöf M, Thiemermann C, Foster SJ, et al. Peptidoglycan primes for LPS-induced release of proinflammatory cytokines in whole human blood. Shock 2001;16:178–82.
[14] Wray GM, Foster SJ, Hinds CJ, Thiemermann C. A cell wall component from pathogenic and non-pathogenic gram-positive bacteria (peptidoglycan) synergises with endotoxin to cause the release of tumor necrosis factor-alpha, nitric oxide production, shock, and multiple organ injury/dysfunction in the rat. Shock 2001;15:135–42.
[15] Yang S, Tamai R, Akashi S, Takeuchi O, Akira S, Sugawara S, et al. Synergistic effect of muramyldipeptide with lipopolysaccharide or lipoteinchoic acid to induce inflammatory cytokines in human monocytic cells in culture. Infect Immun 2001;69:2045–53.
[16] Wolfert MA, Murray TF, Boons G-J, Moore JN. The origin of the synergistic effect of muramyl depeptide with endotoxin and peptidoglycan. J Biol Chem 2002;277:19186–39179.
[17] Wang JE, Dahle MK, McDonald M, Foster SJ, Aasen AO, Tiemermann C. Peptidoglycan and lipoteinchoic acid in gram-positive bacterial sepsis: receptors, signal transduction, biological effects, and synergism. Shock 2003;20:402–14.
[18] Wang JE, Dahle MK, Yndestad A, Bauer I, MsDonald MC, Aukrust P, et al. Peptidoglycan of Staphylococcus aureus causes inflammation and organ injury in the rat. Crit Care Med 2004;32:546–52.
[19] Jiang Q, Akashi S, Miyake K, Petty HR. Cutting edge: Lipopolysaccharide induces physical proximity between CD14 and Toll-like receptor 4 (TLR4) prior to nuclear translocation of NF-κB. J Immunol 2000;165:3541–4.
[20] Flo TH, Halaas Ø, Torp S, Ryan L, Lien E, Dyhdahl B, et al. Differential expression of Toll-like receptor 2 in human cells. J Leukoc Biol 2001;69:474–81.
[21] Matsuda N, Hattori Y, Jesmin S, Gando S. Nuclear factor-κB decoy oligodeoxynucleotides prevent acute lung injury in mice with cecal ligation and puncture-induced sepsis. Mol Pharmacol 2005;67:1018–25.
[22] Morishita R, Sugimoto T, Aoki M, Kita I, Tomita N, Moriguchi A, et al. *In vivo* transfection of *cis* element ''decoy'' against nuclear factor-κB binding site prevents myocardial infarction. Nat Med 1997;8:894–9.
[23] Matsuda N, Hattori Y, Takahashi Y, Nishihira J, Jesmin S, Kobayashi M, et al. Therapeutic effect of in vivo transfection of transcription factor decoy to NF-κB on septic lung in mice. Am J Physiol Lung Cell Mol Physiol 2004;287:L1248–55.
[24] Sirois MG, Jancar S, Braquet P, Plante GE, Sirois P. PAF increases vascular permeability in selected tissues: effect of BN-52021 and L-655,240. Prostaglandins 1988;36:631–44.
[25] Matsuda N, Hattori Y, Gando S, Akaishi Y, Kemmotsu O, Kanno M. Diabetes-induced down-regulation of β_1-adrenoceptor mRNA expression in rat heart. Biochem Pharmacol 1999;58:881–5.
[26] Matsuda N, Hattori Y, Akaishi Y, Suzuki Y, Kemmotsu O, Gando S. Impairment of cardiac β-adrenoceptor cellular signaling by decreased expression of $G_{s\alpha}$ in septic rabbits. Anesthesiology 2000;93:1465–73.
[27] Liu Y, Wang Y, Yamakuchi M, Isowaki S, Nagata E, Kanmura Y, et al. Upregulation of Toll-like receptor 2 gene expression in macrophage response to peptidoglycan and high concentration of lipopolysaccharide is involved in NF-κB activation. Infect Immun 2001;69:2788–96.
[28] Mirlashari MR, Lyberg T. Expression and involvement of Toll-like receptors (TLR)2, TLR4, and CD14 in monocyte TNF-alpha production induced by lipopolysaccharide from Neisseria meningitides. Med Sci Monit 2003;9:BR316–24.
[29] Fan J, Frey RS, Malik AB. TLR4 signaling induces TLR2 expression in endothelial cells via neutrophil NADPH oxidase. J Clin Invest 2003;112:1234–43.
[30] Takeuchi O, Hoshino K, Kawai T, Sanjo H, Takada H, Ogawa T, et al. Differential roles of TLR2 and TLR4 in recognition of gram-negative and gram-positive bacterial cell wall components. Immunity 1999;11:443–51.
[31] Aliprantis AO, Yang RB, Mark MR, Sugget S, Devaux B, Radolf JD, et al. Cell activation and apoptosis by bacterial lipoproteins through toll-like receptor-2. Science 1999;285:736–9.

[32] Dahmash NS, Chowdhury NH, Fayed DF. Septic shock in critically ill patients: aetiology, management and outcomes. J Infect 1993;26:159–70.
[33] Faure E, Thomas L, Xu H, Medvedev A, Equils Q, Arditi M. Bacterial lipopolysaccharide and IFN-γ induce Toll-like receptor 2 and Toll-like receptor 4 expression in human endothelial cells: Role of NF-κB activation. J Immunol 2001;166:2018–24.
[34] Medzhitov R. Toll-like receptors and innate immunity. Nat Rev Immunol 2001;1:135–45.
[35] Sha Q, Truong-Tran AQ, Plitt JR, Beck LA, Schleimer RP. Activation of airway epithelial cells by Toll-like receptor agonists. Am J Respir Cell Mol Biol 2004;31: 358–64.
[36] Droemann D, Goldmann T, Branscheid D, Clark R, Dalhoff K, Zabel P, et al. Toll-like receptor 2 is expressed by alveolar epithelial cells type II and macrophages in the human lung. Histochem Cell Biol 2003;119:103–8.
[37] Armstrong L, Medford ARL, Uppington KM, Robertson J, Witherden IR, Tetley TD, et al. Expression of functional Toll-like receptor-2 and -4 on alveolar epithelial cells. Am J Respir Cell Mol Biol 2004;31:241–5.
[38] Weinstein MP, Towns ML, Quartey SM, Mirrett S, Reimer LG, Parmigiani G, et al. The clinical significance of positive blood culture in the 1990s: a prospective comprehensive evaluation of the microbiology, epidemiology, and outcome of bacteremia and fungemia in adults. Clin Infect Dis 1997;24:584–602.